MICHIGAN STATE UNIVERSITY

CYCLOTRON LABORATORY

"BREAKUP-FUSION" OF ^{7}Li

H. UTSUNOMIYA, S. KUBONO, M.H. TANAKA, M. SUGITANI,

K. MORITA, T. NOMURA and Y. HAMAJIMA

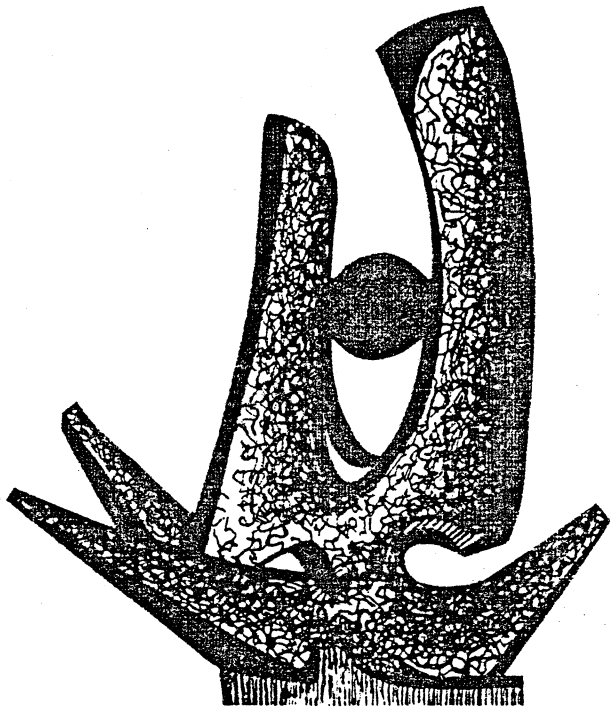

JUNE 1983

MSUCL-420

MSUCL-420
June 1983

"BREAKUP-FUSION" OF ^{7}Li

H. Utsunomiya,* S. Kubono, M.H. Tanaka,
M. Sugitani, and K. Morita**

Institute for Nuclear Study, University of Tokyo
Tanashi, Tokyo, 188 Japan

and

T. Nomura

Cyclotron Laboratory,
The Institute of Physical and Chemical Research
Wako-shi, Saitama, 351 Japan

and

Y. Hamajima

Faculty of Science, Tokyo Metropolitan University
Setagaya, Tokyo, 158 Japan

ABSTRACT

A break-up process of ^{7}Li has been studied by performing the following measurements with 77 MeV ^{7}Li beam; (i) energy and angular distributions of z = 1, 2 particles in the ^{159}Tb + ^{7}Li reaction measured in singles and in coincidence with γ-rays from some heavy residual nuclei, (ii) out-of-plane angular distributions of γ-rays taken in coincidence with α-particles in the ^{159}Tb(^{7}Li,αxn)$^{162-x}$Dy reaction to deduce the spin alignment involved, and (iii) in-plane and out-of-plane angular distributions of fission fragments measured in coincidence with z = 1 and 2 particles emitted in the reaction of ^{232}Th(^{7}Li,xf) to extract the magnitude and alignment of the transferred angular momenta.

The observed energy spectrum of triton and α-particle measured at forward angles exhibits a broad bump centered at a kinetic energy corresponding to the beam velocity, which is characteristic of the break-up mechanism. Roughly a half of the yield at this bump has been shown to originate from a breakup-fusion process, in which one of the breakup fragments is captured by a target nucleus. It is also shown that angular momenta transferred to residual nuclei by breakup-fusion are well aligned along the

normal to the reaction plane and have the magnitude, on the average, consistent with a direct reaction process occurring at the surface region of projectile and target nuclei.

NUCLEAR REACTIONS $^{159}Tb(^{7}Li,x)$, $(^{7}Li,\alpha xn)$, E = 77 MeV; measured $\sigma(E_x,\theta_x)$, α-γ coin., angular correlations $W(\theta_\gamma)$ of discrete γ-rays; deduced $\sigma(E_\alpha)$ in coin. with final nuclei; $^{232}Th(^{7}Li,xf)$, E = 77 MeV; measured x-f angular correlations; deduced magnitude and alignment of average J. Average ℓ for particle emission.

I. INTRODUCTION

The elastic and inelastic break-up of a projectile nucleus by the nuclear or Coulomb force has so far been investigated for various projectiles such as d, $^{3,4}He$, $^{6,7}Li$, ^{9}Be, and $^{10,11}B$.[1-16] The fragmentation of heavier projectiles like ^{16}O and ^{20}Ne has also been reported to take place at incident energies of a few tens of MeV per nucleon.[17-20] The following classification is often used for the projectile break-up processes;[11,21] (i) sequential break-up (decay), which means that an excited projectile resulting from an inelastic reaction decays from well-defined discrete states; (ii) direct break-up, where projectile break up into two or more fragments via virtually excited continuum states and all of these fragments emerge in the exit channel; and (iii) break-up of projectile characterized by the capture of a part of the fragments by a target nucleus. In this paper the "break-up" will not be referred to for phenomena belonging to the first category in order to avoid misunderstanding.

A main purpose of this paper is to study phenomena corresponding to the third process mentioned above, which is called "breakup-fusion" throughout this work. A composite heavy nucleus produced in the breakup-fusion process disintegrates via evaporation of light particles as well as by fission, while a fragment not captured by

the target nucleus behaves as a spectator and moves away approximately with the beam velocity. The experimental[11,22-26] and theoretical[13,27-30] works on such phenomena have so far been done mainly for light particles up to beryllium, although several authors[31-35] have recently paid attention to relation of the breakup-fusion process with "fast" α-particle emission[36-41] observed in reactions induced by heavier projectiles.

A ^{7}Li projectile is considered suitable for the study of breakup-fusion because it has a well-developed cluster structure of an α-particle and a triton. In the present work we have made inclusive and exclusive measurements on energy spectra of light particles emitted in the 77 MeV ^{7}Li bombardment on ^{159}Tb and ^{232}Th. The results clearly indicate the existence of the breakup-fusion process. Out-of-plane angular distributions of γ-rays resulting from breakup-fusion have been measured to extract the spin alignment in residual nuclei produced in this process. We have also measured angular correlations in the ^{232}Th(^{7}Li,xf) reaction (x = p,d,t,α) and discuss the average magnitude and alignment of the transferred angular momenta as well as entrance angular momenta relevant to the breakup-fusion process.

Section II is devoted to the experimental method. The results are presented in Sec. III. The measured spectra, γ-ray angular distributions, and angular

correlations with fission fragments will be analyzed and discussed in Sec. IV. The summary of this work is given in Sec. V.

II. EXPERIMENTAL

The present experiment consists of the following measurements performed with a 77-MeV ^{7}Li beam from SF-cyclotron at the Institute for Nuclear Study; (i) energy and angular distributions of charged particles taken in singles in the bombardment of ^{159}Tb with ^{7}Li projectiles, (ii) energy spectra of α-particles associated with the ^{159}Tb(^{7}Li,αxn)$^{162-x}$Dy reaction, (iii) out-of-plane angular distributions of some discrete γ-rays measured in coincidence with α-particles in the ^{159}Tb(^{7}Li,αxn)$^{162-x}$Dy reaction, and (iv) in-plane and out-of-plane angular distributions of fission fragments measured in coincidence with z = 1,2 particles in the ^{232}Th(^{7}Li,xf) reaction, where x = p,d,t, or α.

The targets used were a self-supporting ^{159}Tb metallic foil of 3.2 mg/cm^{2} thickness and about 500 μg/cm^{2} thick ^{232}Th electrodeposited onto an aluminum foil. Charged particles were detected with several ΔE-E counter telescopes, each consisting of 50 and 5000 μm-thick Si surface barrier detectors. The maximum measurable energies were 30 MeV for protons, 40 MeV for deuterons, 48 MeV for tritons,

and 120 MeV for α-particles. The raw data were recorded event by event on magnetic tapes to be analyzed off line.

Inclusive measurements of energy spectra and angular distributions of z = 1,2 particles were carried out over the angular range 10° to 160°, almost in steps of 5°. The α-γ coincidence measurements were performed using a 91 cm^3 Ge(Li) detector placed 110 mm apart from the target at 90° with respect to the beam direction. α-particles were detected at 30° and 60° with the half angle acceptance of 3.6° and 5.1°, respectively. Figure 1 shows γ-ray spectra measured in coincidence with those α-particles. Prominent γ-ray peaks were found to originate from $^{162-x}$Dy with $2 \leq x \leq 6$ produced in the (^{7}Li,αxn) reaction. For the measurement of out-of-plane angular distributions of discrete γ-rays, the following γ-rays were used: for α emission at 30°, 297.2 keV (^{160}Dy: $6^+ - 4^+$), 210.4 keV (^{159}Dy: $17^+/2 - 13^+/2$), 218.4 keV (^{158}Dy: $4^+ - 2^+$), and 311.2 keV (^{157}Dy: $21^+/2 - 17^+/2$); while for α emission at 60°, 197.0 keV (^{157}Dy: $17^+/2 - 13^+/2$) and 266.3 keV (^{156}Dy: $4^+ - 2^+$) in addition to the 218.4 keV γ-ray from ^{158}Dy as listed above. It should be noted that for α emission at 30° the $4^+ - 2^+$ γ-ray of ^{160}Dy and the $17^+/2 - 13^+/2$ γ-ray of ^{157}Dy were not resolved well from each other, while for α emission at 60° γ-ray yields from ^{160}Dy and ^{159}Dy, produced in the α2n and α3n channels, respectively, were far smaller than those from ^{158,157,156}Dy

as seen in Fig. 1. We defined a reaction plane by the beam and the α-particles and measured out-of-plane angular distributions of the γ-rays in a plane perpendicular to the beam by pivoting a target chamber about the beam axis instead of moving the Ge(Li) detector. The half angle acceptance of the γ counter was 11.8°.

Simultaneous measurements of in-plane and out-of-plane angular distributions of fission fragments were performed in coincidence with hydrogen isotopes and α-particles as follows. As for a detection of the charged particles, a pair of identical Si ΔE-E telescopes were placed at 20° with respect to the beam; one is in a horizontal plane and the other in a verticle plane containing the beam axis. On the other hand, fission fragments were detected with four thin (30 μm) solid state detectors mounted at 95°, 125°, 155°, and 170° in the horizontal plane. Since an aluminum absorber of 600 μm thickness is inserted in front of each ΔE detector in order to eliminate elastically scattered ^{7}Li, the minimum detectable energy was 10 MeV for protons, 14 MeV for deuterons, 16 MeV for tritons, and 40 MeV for α-particles. The half angle acceptance of the fission counters was 2.3°-3.7°. A relative normalization among the four fission counters was made by measuring fission fragments in singles at the same angles.

III. EXPERIMENTAL RESULTS

A. Energy and angular distributions

Figure 2 shows energy spectra of protons, deuterons, tritons, and α-particles observed in singles at various angles in the $^{159}Tb + ^{7}Li$ reaction at 77 MeV. Prominent bumps centered around an energy corresponding to the beam velocity were clearly seen in the spectra taken at small angles, especially for the case of tritons and α-particles. This can be considered as a characteristic feature of the break-up of ^{7}Li as will be described later. The yields of tritons and α-particles at this bump rapidly decrease with the increase of emission angles and merge into a "background", which arises from other origins such as disintegration of highly excited reaction products (a compound nucleus, for instance) and possible preequilibrium emission.

The energy at the peak ($\hat{E}$) and the full width at half-maximum (σ_{FWHM}) in the measured energy distributions for α-particles and tritons as a function of the emission angles are shown in Figs. 3 and 4. The values of σ_{FWHM} at angles larger than 30° are not shown because they are appreciably broadened due to the "background" mentioned above, especially for the case of α-particles. The average value of $\hat{E}$ at the most forward two angles observed in this experiment is about 44.4 MeV for α-particles and 30.4 MeV for tritons. In a naive picture of the

break-up process, the projectile energy is first used to separate α- and t- clusters in ^{7}Li and the rest of the kinetic energy is shared by α-particle and triton in proportion to their mass numbers. Because the above separation energy is 2.47 MeV, this yields 42.6 MeV for α-particle and 31.9 MeV for triton, being close to the observed $\hat{E}$ values. The Coulomb energy difference between the entrance and exit channels as well as the angle dependence of $\hat{E}$ will be described in Sec. IVA. The value of σ_{FWHM} lies around 17.5 MeV both for α-particle and triton. This will be reasonably well accounted for by a simple semi-classical treatment of the break-up process in Sec. IVA.

Figure 5 shows angular distributions of z = 1 and 2 particles measured in the $^{159}Tb + ^{7}Li$ reaction at 77 MeV. At small angles the cross sections of α-particles and tritons are much larger than those of deuterons and protons. This must be, at least partly, due to large contributions of the break-up of ^{7}Li into α + t. Another interesting feature is that the yield of the beam velocity α-particles is about three times as large as that of the beam velocity tritons. There are at least three reasons for this fact: (i) Because the binding energy of a triton is much smaller than that of an α-particle, the triton arising from break-up of ^{7}Li

may further break up into two neutrons and a proton or into a neutron and a deuteron with the interaction of the nuclear field. In fact, the energy spectra of protons and deuterons at forward angles given in Fig. 2 indicate bumps at energies nearly corresponding to the beam velocity though they are not so prominent as the case of α-particles and deuterons. (ii) A partner of the break-up fragment can be captured by a target nucleus (breakup-fusion) as will be seen in Sec. IIIB. This may be considered as a triton- or α-transfer reaction. The Q-value for the $^{159}Tb(^{7}Li,\alpha)^{162}Dy$ reaction is 11.1 MeV, while it is -3.2 MeV for the $(^{7}Li,t)$ reaction, indicating that the α-particle emission is more favored. (iii) The sequential-breakup of a projectile-like fragment may favor α-particle emission. For example, Casteneda et al.[24] reported that in the ^{6}Li-induced reactions, the sequential decay of the ground state of ^{5}Li into an α-particle and a proton partly contributes to production of α-particles.

B. Out-of-plane γ-ray angular distributions

Figure 6 shows energy spectra of α-particles associated with the reaction channel of $^{159}Tb(^{7}Li,\alpha xn)^{162-x}Dy$, which have been measured at 30° and 60° in coincidence with discrete γ-rays as described in Section II. The dominant channel at 30° turned out to be the $(^{7}Li,\alpha 4n)$

reaction, for which the α-particle spectrum was nearly centered around the beam-velocity energy, while the α5n and α6n channels became more significant at 60°. Because of poor statistics an α-particle spectrum for the α6n channel could not be obtained at 30°. Energy spectra taken in singles and in coincidence with any γ-rays entering the γ-ray detector are also given by dotted and solid curves in Fig. 6, respectively. For convenience, they are normalized at the low energy side of the α-particle spectra. Note that roughly a half of the beam velocity α-particles measured in singles at 30° was rejected by the "γ-ray multiplicity filter" in the α-γ measurement. This is a consequence of the fact that the "filter" excludes such events as direct- and sequential-breakup of ^{7}Li because of their very low γ-ray multiplicities. In other words, about a half of the beam velocity α-particles at 30° correspond to the breakup-fusion reaction, in which tritons are captured by a target nucleus.

Out-of-plane angular distributions ($W(\theta_\gamma)$) of the discrete γ-rays measured in coincidence with α-particles at 30° and 60° are shown in Figs. 7 and 8. The data are normalized such that the values of W(0°) are equal to 1.0. The symbol θ_γ denotes a polar angle of the γ-ray counter with respect to the quantization z-axis, which is chosen along the normal to the reaction plane. The yield ratio of the in-plane to out-of-plane intensity,

$R = W(90°)/W(0°)$, is roughly equal to 2 for the $\alpha 2n$, $\alpha 3n$, and $\alpha 4n$ channels, while it is around 1.2 for the $\alpha 5n$ and $\alpha 6n$ channels. This suggests that the spin alignment in residual nuclei is large for high-energy α-particle emission, while it is smaller in the case of low-energy α-particle emission. A quantitative deduction of the spin alignment will be described in Sec. IVC.

C. Light particle-fission fragment angular correlations

Figure 9 shows energy spectra of z = 1 and 2 particles obtained at 20° in coincidence with fission fragments in the $^{232}Th(^{7}Li,xf)$ reaction. The given energies are those in the center-of-mass system, which has been transformed from the laboratory spectra by assuming a binary reaction process like $^{7}Li + ^{232}Th \rightarrow x + F$, where x and F denote a measured light particle and a residual fissile nucleus, respectively. The cut-off of the low-energy side of the spectra was due to the Al foil inserted before the particle detectors as mentioned in Section II.

Figure 10 shows in-plane and out-of-plane angular distributions of fission fragments measured in coincidence with z = 1 and 2 particles. The geometry of describing the angular correlations was taken to be the same as in Ref. 42; the z-axis was chosen along the normal to the reaction plane which was determined by the direction of the beam and the measured light particles, while the

x-axis was taken along the average recoil angle (ψ_R) of a fissile nucleus which was determined by the average kinetic energy and the emission angle of each light particle, the y-axis being perpendicular to both x- and z-axes. Average values of the measured kinetic energies are 15.0 MeV for protons, 21.3 MeV for deuterons, 27.1 MeV for tritons, and 47.6 MeV for α-particles, yielding $\psi_R = 3.9°$ for protons, $\psi_R = 7.4°$ for deuterons, $\psi_R = 11.8°$ for tritons, and $\psi_R = 24.7°$ for α-particles. θ and φ denote polar and azimuthal angles, respectively. The measurements of out-of-plane angular distributions were made at $\phi_{lab} = 184°$ for protons, $\phi_{lab} = 187°$ for deuterons, $\phi_{lab} = 192°$ for tritons, and $\phi_{lab} = 205°$ for α-particles. The measured in-plane angular distributions were peaked almost at the recoil angle of the fissile nucleus, suggesting that angular momenta transferred to the fissioning nucleus preferentially lie in the y-z plane. The in-plane anisotropies for α-f and t-f correlations are smaller than those for p-f and d-f correlations. This indicates that the spin alignment in residual nuclei produced by α-particle or triton emission is larger than that of nuclei produced by proton or deuteron emission.

An analysis of the angular correlations will be described in the next section.

IV. ANALYSIS AND DISCUSSION

A. The peak energy and FWHM in singles spectra

A purpose of this section is to show that some features of the inclusive energy spectra of α-particles and tritons are reasonably well explained by a simple treatment of the break-up process. We will be satisfied with rough agreement between experiment and theory because the experimental quality appears insufficient for the detailed comparison, and will focus on the peak energy and the full width at half-maximum shown in Figs. 3 and 4.

We shall first follow a plane-wave approximation of Serber,[43] who treated the elastic break-up of deuteron at the 190-MeV incident energy in a semi-classical model. Expressing an internal motion with a wave function of the Yukawa type, he calculated cross section, energy, and angular distributions of neutron emission with the assumption that a target nucleus is either transparent or opaque to neutrons. Let us now consider the break-up of a projectile nucleus a into b plus c, i.e.,

$$a \rightarrow b + c \qquad (1)$$

in complete analogy with Ref. 43. Then, a laboratory energy spectrum at very forward angles can be written in the case of an opaque nucleus by

$$N(E_x) \propto E_a\sqrt{\epsilon}/[(E_x - \frac{A_x}{A_a}E_a)^2 + \frac{4A_bA_c}{A_a^2}\epsilon E_a]^{3/2} , \qquad (2)$$

where x denotes b or c, E_a is the projectile energy, etc., A_x is the mass number of a nucleus x, etc., and ε is the separation energy of b and c in the nucleus a. An opaque-nucleus approximation has been adopted here because the projectile of present interest is ^{7}Li of low energy. It is easy to see that Eq. (2) yields $\hat{E}_x = A_xE_a/A_a$ and $\sigma_{FWHM} = 3.066\ (A_bA_c\epsilon E_a)^{1/2}/A_a$. Since the Coulomb energy difference mentioned in Section III is not included in Eq. (2), we take this effect into account in the same way as in Ref. 8; that is, E_a in Eq. (2) is replaced with the projectile energy reduced by the Coulomb potential in the entrance channel, and E_x in Eq. (2) is replaced with the energy of x before the Coulomb acceleration in the exit channel. Then, we obtain

$$\hat{E}_x = A_xE_a/A_a + (Z_x - A_xZ_a/A_a)V^C , \qquad (3)$$

$$\sigma_{FWHM} = 3.066\ (A_bA_c\epsilon E_a)^{1/2}/A_a \times (1 - Z_aV^C/E_a)^{1/2} , \qquad (4)$$

where Z_x is the atomic number of a nucleus x, etc., and V^C is the Coulomb energy per unit charge. By putting ε = 2.47 MeV, V^C = 8 MeV, E_a = 74.5 MeV (see Sec. IIIA), and proper values for A_a, Z_a, etc. in the ^{159}Tb + ^{7}Li reaction, we obtain $\hat{E}_\alpha$ = 44.9 MeV, E_t = 29.6 MeV,

and σ_{FWHM} = 16.9 MeV both for α and t, which compare fairly well with the experimental results.

We shall now consider the angle dependence of $\hat{E}_x$ and σ_{FWHM}. A formula corresponding to Eq. (2) has been derived in Ref. 43 for the case that the direction of a fragment x is almost the same as that of the incident projectile. This is not always the case in the present reaction, because the momentum due to internal motion ($\vec{p}$) is not very small compared with that of the incident motion of the projectile ($\vec{P}_a$). Let the fragment x be deflected by the amount of θ due to the coupling of $\vec{p}$ and $\vec{P}_a$. Then, an energy distribution of x is approximately expressed by Eq. (2) when E_a in this formula is replaced with $E_a\cos^2\theta$. The peak energy and the width are also given by Eqs. (3) and (4), respectively, when $E_a\cos^2\theta$ is used for E_a.

It should be noted, however, that θ does not necessarily correspond to the emission angle θ_L, because the projectile as well as the fragment x after the break-up must be deflected in the Coulomb and nuclear field. If this deflection angle is θ_o, then we have $\theta_L = \theta_o + \theta$. The same procedure has been used in Ref. 17.

It is not possible to determine the value of θ_o only from the above consideration. Experimentally, the peak energy increases with the decrease of emission angles, and becomes almost constant around the angle of 10-15°

for the case of α-particles. As the maximum peak energy is realized at $\theta_L = \theta_o$, we have decided to take θ_o = 10°, and calculated the angular dependence of $\hat{E}_\alpha$, $\hat{E}_t$, and σ_{FWHM} by replacing E_a with $E_a\cos^2(\theta_L - \theta_o)$ in Eqs. (3) and (4). The agreement with the experimental results is quite satisfactory in view of our simple treatment. Note that the measured value of σ_{FWHM} may be overestimated for the case of α-particles due to other components originating from the decay of the compound nucleus, possible pre-equilibrium emission, and so on as mentioned in Section III.

B. Magnitude of the transferred and entrance angular momenta

The angular distributions of fission fragments as shown in Fig. 10 are known to depend on the magnitude and alignment of angular momenta transferred to residual fissioning nuclei produced by light particle emission. We have made the simultaneous fit to the measured in-plane and out-of-plane data using the same semi-classical formalism as described in the literature.[42,44-45]

The analysis depends on the assumption that the final direction of fission fragments is directly related to the orientation of the nuclear symmetry axis during passage over the saddle point.[46] The angular distribution of fission fragments from a nucleus having intrinsic angular momentum J whose projections on the space-fixed

z-axis and the nuclear symmetry axis are M and K, respectively, can be written by

$$W^J_{MK}(\theta) = \frac{1}{2}\,(2J+1)\,|d^J_{MK}(\theta)|^2\,, \qquad (5)$$

where θ is a polar angle and $d^J_{MK}(\theta)$ are rotational wave functions. In order to reproduce the experimental data we have to sum Eq. (5) over J, M, and K with appropriate weight functions. Since Dyer et al.[42] have shown that the experimental angular correlations are sensitive only to the first moment of the J-distribution, we fitted the data by using a single value of J which should be regarded as the average value of the J-distribution. The K-distribution is usually assumed to be given by $\exp(-K^2/2K_o^2)$, where the width parameter K_o can be estimated from the effective moment of inertia and the nuclear temperature at the saddle point. Following the procedure given by Refs. 46 and 47, we have estimated, in the present ^{232}Th(^{7}Li,xf) reaction, K_o to be 11 ħ for x = proton, deuteron, and triton, and K_o 10 ħ for α-particle. As for the M-distribution, we assume that the angular momentum vector $\vec{J}$ lies in the y-z plane and is expressed in the manner (either (i) or (ii)) given below: (i) (method A) $\vec{J}$ is composed of random coupling of a component $\vec{J}_1$ completely aligned along the z-axis and a component $\vec{J}_2$ uniformly distributed in the y-z

plane, i.e. $\vec{J} = \vec{J}_1 + \vec{J}_2$; (ii) (method B) The polar angle β of $\vec{J}$ is distributed by $\exp(-\beta^2/2\beta_o^2)$. The fitting parameters are magnitudes of $\vec{J}$ and $\vec{J}_2$ by method A and the magnitudes of J and β_o by method B. More details have been described elsewhere.[42,44-45]

Examples of the best fits are shown by solid curves in Fig. 10. The best-fit parameters are listed in Table I. The resultant spin alignment has been calculated by

$$P_{zz} = \frac{3\langle M^2\rangle}{2\langle J^2\rangle} - \frac{1}{2}\,. \qquad (6)$$

Note that $P_{zz} = 1$ if $\vec{J}$ is completely aligned along the z-axis, $P_{zz} = 0.25$ if $\vec{J}$ is randomly distributed in the y-z plane. The following points should be noted. (i) The K_o dependence of the fitting parameters was examined by analyzing the same data with K_o = 10 ħ and K_o = 12 ħ for p, d, and t, and with K_o = 9 ħ and K_o = 11 ħ for α; the resultant change of J and P_{zz} was 2-3 ħ and 3-4%, respectively. (ii) The deduced value of J tends to increase linearly with the decrease of the observed ejectile mass as shown in Fig. 11. This suggests that the rest of the projectile is captured by a target nucleus, and that the magnitude of the transferred angular momenta is nearly proportional to the mass number of the captured fragment. (iii) The value of P_{zz} for triton- and α-particle emission

is much larger than that for proton- and deuteron emission.

The present experimental data were taken at 20° for the light-particle emission, where the break-up process played an important role, at least for α-particles and tritons. The particle energies involved in the measurement also correspond to the region in which the contribution of the break-up is dominant, although the peak energies appear somewhat lower than those expected in the inclusive spectra (see Fig. 9). It is therefore interesting to estimate an average value of entrance angular momenta (ℓ_i) to see if it is consistent with the "breakup-fusion" of ^{7}Li. For this purpose, we assume that the entrance angular momenta of ^{7}Li are shared between α-particle and triton in the break-up process, and that they are transferred to the residual fissioning nuclei in the (^{7}Li,tf) and (^{7}Li,αf) reactions. Then, taking the sum of the J-values deduced for triton and α-particle emissions, we obtain ℓ_i to be 41 ± 6 ħ (method A) or 43 ± 7ħ(method B) for the break-up fusion of ^{7}Li. We have here neglected possible contribution of neutron evaporation before the fission takes place as well as intrinsic angular momenta of the fission fragments. The grazing angular momentum (ℓ_{gr}) of the ^{232}Th + ^{7}Li reaction at 77 MeV is 44 ħ, while the critical angular momentum for complete fusion (ℓ_{cr}) is estimated to be

38 ħ from a model of Bass.[48] Therefore, the above values of ℓ_i are likely to be close to ℓ_{gr} or to lie between ℓ_{cr} and ℓ_{gr}.

Another simple estimate of ℓ_i for the (^{7}Li,αf) and (^{7}Li,tf) reactions may be based on the assumption that ℓ_i is divided into α and t in proportion to their masses. Then, it is possible to estimate ℓ_i for the α-particle and triton emission separately, because $\ell_i \simeq 7J/3$ for the (^{7}Li,αf) reaction and $\ell_i \simeq 7J/4$ for (^{7}Li,tf). This assumption yields $\ell_i \simeq 49 \pm 9$ ħ for the former and $\ell_i \simeq 37 \pm 9$ ħ for the latter. (The average values deduced from methods A and B are used here.)

Recently, similar α-f angular correlations have been measured in the bombardment of ^{209}Bi with ^{14}N-, ^{16}O-, and ^{20}Ne-projectiles at the incident energy of 7-8 MeV per nucleon to deduce the magnitude of the transferred angular momenta.[45,49] The results clearly indicate $\ell_i < \ell_{cr}$ for the energetic α-particle emission, being in strong contrast with the present result discussed above. The energy spectra reported in Refs. 45 and 49 appear Maxwellian with high temperature even at forward angles, though more energetic than expected in the compound reaction. These facts suggest that the precompound emission is dominant in such heavy-ion reactions at low bombarding energies smaller than 10 MeV/amu, while the present result is more consistent with a direct reaction

taking place in the peripheral region, although the above two reaction processes must be, in principle, internally related to each other. Udagawa et al.[50] have recently predicted that the breakup-fusion takes place with partial waves of angular momenta considerably smaller than ℓ_{gr}. The present result seems consistent with their result, though relatively large errors of the estimated ℓ_i values prevent us from a clear conclusion.

The ℓ_i values for the proton and deuteron emission can be estimated if we assume again that ℓ_i is divided in proportion to the masses of the captured and detected fragments provided all the rest of the projectile is transferred to a target nucleus. Taking the average values of J given in Table I, the above assumption leads to $\ell_i = 40 \pm 9\ \hbar$ and $\ell_i = 39 \pm 9\ \hbar$ for the (^{7}Li,pf) and (^{7}Li,df) reactions, respectively. However, the experimental energy spectra for these particles lie in the region where the compound-nucleus decay as well as preequilibrium emission are significant, throwing some doubt on the above assumption. A more detailed study will be necessary to elucidate this point.

C. Spin alignment

The measured out-of-plane angular distributions of discrete γ-rays in the ^{159}Tb(^{7}Li,αxn)$^{162-x}$Dy reaction have been analyzed by following the prescription of

Refs. 51 and 52. We assume that the distribution of the magnetic-substate population W(M) (M = -J,...,J) for an initial state with spin J, which emits the γ-ray of interest, is Gaussian[53]; that is,

$$W(M) \propto \exp[-(J - M)^2/2\sigma_M^2] \ . \qquad (7)$$

Note that the quantization (z-) axis is chosen along the normal to the reaction plane. Then, the angular distributions of γ-rays with respect to the z-axis can be written in the usual manner as described in the literature.[52]

The width σ_M has been treated as a unique adjustable parameter in order to reproduce the experimental data. The best fits are shown by solid curves in Figs. 7 and 8. The best-fit parameters are listed in Table II together with the resultant spin alignment along the z-axis, which is calculated from

$$P_{zz} = \frac{3\langle M^2\rangle - J(J+1)}{J(2J-1)} \ , \qquad (8)$$

by following Ref. 54. Note that this formula for P_{zz} is slightly different from Eq. (6), but becomes almost the same when J is large. Since the spin value of J involved in this section is small and well defined, we consider Eq. (8) as a better expression for the spin alignment.

The following points should be noted: (i) The deduced spin alignment depends essentially on the reaction

channels, but seems nearly independent of the present emission angles of 30° and 60°. (ii) The deduced values of P_{zz} (=0.56 - 0.62) for the α2n, α3n, and α4n channels associated with high-energy α-particles are much larger than those for the α5n and α6n channels associated with low-energy α-particles, where the P_{zz} values lie between 0.15 and 0.33 which are close to an expectation value of P_{zz} = 0.25 in the case of a compound nucleus.

It should be noted that the P_{zz} values deduced above are those for the γ-ray emitting states. If we want to transform them to the alignment after the α-particle emission, we have to correct attenuation of the alignment due to neutron and γ-ray emission before reaching the states involved in the analysis. Because this correction is usually expected not to be very large if angular momenta of the initial states are large,[51,52] we will not attempt to correct the above attenuation, and assume that the deduced values of P_{zz} are close to the spin alignment after the α-particle emission. This seems to be supported by the fact that the P_{zz} values for the α2n, α3n, and α4n channels corresponding to high-energy α-particle emission are nearly equal to P_{zz} for α given in Table I. There may exist another cause for the attenuation of the spin alignment due to an interaction of magnetic and electric fields in a solid terbium target. Although this effect is difficult to estimate, it is presumably small

because lifetimes of the states involved are not particularly long.

The large spin alignment for the α2n, α3n, and α4n channels pointed out above is consistent with the fact that the high-energy α-particle emission mainly originates from a direct reaction (breakup-fusion). On the other hand, the low-energy α-particle emission leading to the α5n and α6n channels includes the decay of the compound nucleus dominantly, being also consistent with the small alignment observed. However, the above fact cannot be considered as an evidence for the difference of the reaction mechanism, as there may be another reason, as described below, for the difference of the observed P_{zz} values. Assume that α-particles are emitted from the compound nucleus whose intrinsic angular momenta ($\vec{J}_c$) are randomly distributed in a plane perpendicular to the beam direction. The α-particles also carry relative angular momenta ($\vec{J}_\alpha$) lying in another plane perpendicular to their direction. The intersection of the above two planes is the z-axis, which is realized in the case of the "stretched transition", i.e., $\vec{J}_\alpha$ // $\vec{J}_c$. Note that this is the most probable even in the decay of the compound nucleus due to the spin dependence of the level density, and becomes dominant when J_α becomes large. If we note that high-energy α-particles tend to carry large values of J_α, the energy dependence of P_{zz} presently

deduced may occur even in the compound reaction. The small P_{zz} values for the proton and deuteron emission given in Table I may also be ascribed to the fact that these particles carry small angular momenta.

V. SUMMARY

Energy spectra of α-particles and tritons measured at forward angles in the $^{159}Tb + ^{7}Li$ reaction at 77 MeV exhibit prominent bumps centered around an energy corresponding to the beam velocity. The peak energy and the full width at half-maximum of this bump are reasonably well accounted for by a simple semi-classical treatment of the break-up of ^{7}Li. Roughly a half of the yield at this bump for α-particles measured at 30° corresponds to the breakup-fusion reaction, in which the other breakup-fragment (triton) is captured by a target nucleus. The average magnitude of entrance angular momenta relevant to the breakup-fusion reaction estimated from angular correlations of fission fragments in the $^{232}Th(^{7}Li,xf)$ reaction at 77 MeV is close to the grazing angular momentum, being consistent with a value expected from a direct reaction taking place in a peripheral region. The large spin alignment has been deduced for heavy residual nuclei produced in the above process.

ACKNOWLEDGEMENTS

The authors are very grateful to the staff of the INS machine shop for their help in constucting a target chamber suitable for the particle-γ coincident experiment. We would like to thank Professor M. Ichimura for helpful discussion. One of us (H.U.) would like to thank Professor H. Kamitsubo for the kind hospitality extended to him during his stay at IPCR, where a part of this manuscript has been prepared.

REFERENCES

*Present address: National Superconducting Cyclotron Laboratory, Michigan State University, East Lansing, MI 48824, USA

**On leave from Kyushu University, Fukuoka 812 Japan

1. J.R. Wu, C.C. Chang, and H.D. Holmgren, Phys. Rev. C19, 370 (1979).
2. U. Bechstedt, H. Machner, G. Bauer, R. Shyam, C. Alderliesten, O. Bousshid, A. Djaloeis, P. Jahn, C. Mayer-Böricke, F. Rösel, and D. Trautmann, Nucl. Phys. A343, 221 (1980).
3. F. Udo, Rev. Mod. Phys. 37, 365 (1965).
4. E.C. May, B.L. Cohen, and T.M. O'Keffe, Phys. Rev. 164, 1253 (1967).
5. E.W. Hamburger, B.L. Cohen, and R.E. Price, Phys. Rev. 121, 1143 (1961).
6. J. Pampus, J. Bisplinghoff, J. Ernst, T. Mayer-Kuckuk, J. Rama Rao, G. Baur, F. Rösel, and D. Trautmann, Nucl. Phys. A311, 141 (1978).
7. A. Chevarier, N. Chevarier, A. Demeyer, A. Alevra, I.R. Lukas, M.T. Magda, and M.E. Nistor, Nucl. Phys. A237, 354 (1975).

8. N. Matsuoka, A. Shimizu, K. Hosono, T. Saito, M. Kondo, H. Sakaguchi, Y. Toba, A. Goto, F. Ohtani, and N. Nakanishi, Nucl. Phys. A311, 173 (1978); N. Matsuoka, A. Shimizu, K. Hosono, T. Saito, M. Kondo, H. Sakaguchi, A. Goto, and F. Ohtani, Nucl. Phys. A337, 269 (1980).
9. J.R. Wu, C.C. Chang, and H.D. Holmgren, Phys. Rev. Lett. 40, 1013 (1978).
10. A. Budzanowski, G. Baur, C. Alderliesten, J. Bojowald, C. Mayer-Böricke, W. Oelert, and P. Turek, Phys. Rev. Lett. 41, 635 (1978).
11. R.W. Koontz, C.C. Chang, H.D. Holmgren, and J.R. Wu, Phys. Rev. Lett. 43, 1862 (1979).
12. B. Neumann, H. Rebel, H.J. Gils, R. Planeta, J. Buschmann, H. Klewe-Nebenius, S. Zagromski, R. Shyam, and H. Machner, Nucl. Phys. A382, 296 (1982).
13. K.O. Pfeiffer, E. Speth, and K. Bethge, Nucl. Phys. A206, 545 (1973).
14. R.W. Ollerhead, C. Chasman, and D.A. Bromley, Phys. Rev. 134, B74 (1964).
15. J. Unternährer, J. Lang, and R. Müller, Phys. Rev. Lett. 40, 1077 (1978).
16. G. Baur, M. Pauli, F. Rösel, and D. Trautmann, Nucl. Phys. A315, 241 (1979).

17. C.K. Gelbke, D.K. Scott, M. Bini, D.L. Hendrie, J.L. Laville, J. Mahoney, M.C. Mermaz, and C. Olmer, Phys. Lett. 70B, 415 (1977).

18. Ch. Egelhaaf, G. Bohlen, H. Fuchs, A. Gamp, H. Homeyer, and H. Kluge, Phys. Rev. Lett. 46, 813 (1981).

19. B.G. Harvey, Phys. Rev. Lett. (Comments) 47, 454 (1981).

20. J.B. Natowitz, M.N. Namboodiri, L. Adler, R.P. Schmitt, R.L. Watson, S. Simon, M. Berlanger, and R. Choudhury, Phys. Rev. Lett. 47, 1114 (1981).

21. J.R. Wu and I.Y. Lee, Phys. Rev. Lett. 45, 8 (1980).

22. J. Kropp, H. Klewe-Nebenius, and H. Faust, J. Beschmann, H. Rebel, H.J. Gils, and K. Wisshak, Z. Phys. A280, 61 (1977).

23. J.G. Fleissner, D.A. Rakel, F.P. Venezia, E.G. Funk, J.W. Mihelich, and H.A. Smith, Jr., Phys. Rev. C17, 1001 (1978).

24. C.M. Castaneda, H.A. Smith, Jr., T.E. Ward, and T.R. Nees, Phys. Rev. C16, 1437 (1977); C.M. Castaneda, H.A. Smith, Jr., P.P. Singh, J. Jastrzebski, H. Karwowski, A.K. Gaigalas, Phys. Lett. 77B, 371 (1978); C.M. Castaneda, H.A. Smith, Jr., P.P. Singh, and H. Karwowski, Phys. Rev. C21, 179 (1980).

25. H. Freiesleben, H.C. Britt, J. Birkelund, and J.R. Huizenga, Phys. Rev. C10, 245 (1974).

26. B. Neumann, J. Buschmann, H. Klewe-Nebenius, H. Rebel, and H.J. Gils, Nucl. Phys. A329, 259 (1979).

27. M. Kawai, A.K. Kerman, and K.W. McVoy, Ann. Phys. (NY) 75, 156 (1973).

28. A.K. Kerman and K.W. McVoy, Ann. Phys. (NY) 122, 197 (1979).

29. G. Baur, F. Rösel, D. Trautmann, and R. Shyam, Continuum Spectra on Heavy Ion Reaction, edited by T. Tamura, J.B. Natowitz, and D.H. Youngblood (Harwood Acad. Pub., 1980), p. 131.

30. N. Austern and C.M. Vincent, Phys. Rev. C23, 1847 (1981).

31. T. Kishimoto and K.-I. Kubo, Proc. of Symp. on High Spin Phenomena in Nuclei, 1979, Argonne, ANL/Phy-79-4, 535 (1979).

32. T. Udagawa and T. Tamura, Phys. Rev. Lett. 45, 1311 (1980).

33. M. Ichimura, E. Takada, T. Yamaya, and K. Nagatani, Phys. Lett. 101B, 31 (1981).

34. D.R. Zolnowski, H. Yamada, S.E. Cala, A.C. Kahler, and T.T. Sugihara, Phys. Rev. Lett. 41, 92 (1978).

35. E. Takada, T. Shimoda, N. Takahashi, T. Yamaya, K. Nagatani, T. Udagawa, and T. Tamura, Phys. Rev. C23, 772 (1981).

36. H.C. Britt and A.R. Quinton, Phys. Rev. 124, 877 (1961).

37. J. Galin, B. Gatty, D. Guerreau, C. Rouussett, U.C. Schlotthauer-Voos, and X. Tarrago, Phys. Rev. C9, 1126 (1974).

38. T. Inamura, M. Ishihara, T. Fukuda, T. Shimoda, and H. Hiruta, Phys. Lett. 68B, 51 (1977); T. Inamura, T. Kojima, T. Nomura, T. Sugitate, and H. Utsunomiya, Phys. Lett. 84B, 71 (1979).

39. T. Nomura, H. Utsunomiya, T. Motobayashi, T. Inamura, and M. Yanokura, Phys. Rev. Lett. 40, 694 (1978); T. Nomura, H. Utsunomiya, T. Inamura, T. Motobayashi, and T. Sugitate, J. Phys. Soc. Japan 46, 335 (1979); H. Utsunomiya, T. Nomura, T. Inamura, T. Sugitate, and T. Motobayashi, Nucl. Phys. A334, 127 (1980).

40. K. Siwek-Wilczynsky, E.H. du Marchie van Voorthuysen, J. van Popta, R.H. Siemssen, and J. Wilcynski, Phys. Rev. Lett. 42, 1599 (1979).

41. K.A. Geoffroy, D.G. Sarantities, M.L. Halbert, D.C. Hensley, R.A. Dayras, and J.H. Barkes, Phys. Rev. Lett. 43, 1303 (1979).

42. P. Dyer, R. Vandenbosch, R.J. Puigh, T.D. Thomas, and M.S. Zieman, Phys. Rev. Lett. 39, 392 (1977); P. Dyer, R.J. Puigh, R. Vandenbosch, T.C. Thomas, M.S. Zieman, and L. Nunnelley, Nucl. Phys. A322, 205 (1979).

43. R. Serber, Phys. Rev. 72, 1008 (1947).

44. R.J. Puigh, P. Dyer, R. Vandenbosch, T.D. Thomas, L. Nunnelley, and M.S. Zieman, Phys. Lett. 86B, 24 (1979).

45. H. Utsunomiya, T. Nomura, M. Ishihara, T. Sugitate, K. Ieki, and S. Kohmoto, Phys. Lett. 105B, 135 (1981).

46. R. Vandenbosch and J.R. Huizenga, Nuclear Fission (Academic Press, New York, 1973).

47. B.B. Back and S. Bjørnholm, Nucl. Phys. A302, 343 (1978).

48. R. Bass, Nucl. Phys. A231, 45 (1974).

49. H. Utsunomiya, T. Nomura, S. Kohmoto, S. Sasagase, and K. Sueki (to be published).

50. T. Udagawa, D. Price, and T. Tamura (to be published in Phys. Lett.).

51. J.O. Rasmussen and T.T. Sugihara, Phys. Rev. 151, 992 (1966).

52. H. Morinaga and T. Yamazaki, In-beam gamma-ray spectroscopy (North Holland, Amsterdam, New York, Oxford, 1976).

53. H. Puchta, W. Dünnweber, W. Hering, C. Lauterbach, and W. Trautmann, Phys. Rev. Lett. 43, 623 (1979).

54. T. Døssing, Nucl. Phys. A357, 488 (1981).

Table I. The best fit parameters together with the resultant P_{zz} values obtained for the particle-fission fragment angular correlations in the $^{232}Th(^{7}Li,xf)$ (x = p,d,t,α) reaction at 77 MeV, where the particles are detected at 20°. The angular momenta are given in units of ħ and β_o in degrees.

Emitted particles	Method	J	J_2	β_o	P_{zz}
p	A	32 ± 7	31	--	$0.30 \pm {}^{0.02}_{0.01}$
	B	36 ± 8	--	69	$0.39 \pm <0.01$
d	A	37 ± 6	26	--	$0.31 \pm {}^{<0.01}_{0.06}$
	B	29 ± 7	--	71	0.38 ± 0.01
t	A	21 ± 5	17	--	$0.51 \pm {}^{0.10}_{0.16}$
	B	21 ± 6	--	41	$0.56 \pm {}^{0.03}_{0.09}$
α	A	20 ± 4	14	--	$0.63 \pm {}^{0.16}_{0.14}$
	B	22 ± 4	--	35	$0.62 \pm {}^{0.03}_{0.08}$

Table II. The best fit parameters together with the resultant P_{zz} obtained for γ-ray angular distributions in the $^{159}Tb(^{7}Li,\alpha x n\gamma)^{162-x}Dy$ reaction at 77 MeV.

Emission angle of α	Reaction channel	Residual Nucleus	E_γ (keV)	Transition J → J'	σ_M/J	P_{zz}
30°	α2n	^{160}Dy	297.2	$6^+ \rightarrow 4^+$	0.23 ± 0.02	0.62 ± 0.04
	α3n	^{159}Dy	210.4	$17^+/2 \rightarrow 13^+/2$	0.23 ± 0.01	0.60 ± 0.02
	α4n	^{158}Dy	218.4	$4^+ \rightarrow 2^+$	0.26 ± 0.01	0.61 ± 0.02
	α5n	^{157}Dy	311.2	$21^+/2 \rightarrow 17^+/2$	0.37 ± 0.04	0.33 ± 0.05
60°	α4n	^{158}Dy	218.4	$4^+ \rightarrow 2^+$	0.29 ± 0.02	0.56 ± 0.04
	α5n	^{157}Dy	197.0	$17^+/2 \rightarrow 13^+/2$	0.50 ± 0.06	0.24 ± 0.05
	α6n	^{156}Dy	266.3	$4^+ \rightarrow 2^+$	0.71 ± 0.22	0.15 ± 0.10

FIGURE CAPTIONS

Fig. 1. Typical γ-ray spectra observed in coincidence with α-particles emitted at 30° (a) and 60° (b) in the $^{159}Tb + ^{7}Li$ reaction at 77 MeV.

Fig. 2. Some energy spectra of protons, deuterons, tritons, and α-particles observed at various angles in the $^{159}Tb + ^{7}Li$ reaction at 77 MeV. The laboratory angles are indicated.

Fig. 3. Kinetic energies of α-particles at the peak ($\hat{E}_\alpha$) and the full width at half-maximum (σ_α^{FWHM}) of the continuous break-up bumps as a function of emission angles. The solid curves show theoretical values as explained in the text.

Fig. 4. Kinetic energies of tritons at the peak $\hat{E}_t$ and the full width at half-maximum σ_t^{FWHM} of the continuous break-up bumps as a function of emission angles. The solid curves show theoretical values as explained in the text.

Fig. 5. Angular distributions of protons, deuterons, tritons, and α-particles measured in the $^{159}Tb + ^{7}Li$ reaction at 77 MeV.

Fig. 6. Energy spectra of α-particles measured at 30° and 60° for the $^{159}Tb(^{7}Li,\alpha xn)^{162-x}Dy$ reaction channels. The solid curves indicate α spectra measured in coincidence with any γ-rays entering the Ge(Li) detector. The dotted curves show the inclusive energy spectra of α-particles. The dashed curves are to guide the eye.

Fig. 7. Out-of-plane angular distributions of discrete γ-rays from $^{162-x}Dy$ ($2 \leq x \leq 5$) measured in coincidence with α-particles emitted at 30° in the $^{159}Tb(^{7}Li,\alpha xn)^{162-x}Dy$ reaction at 77 MeV. The solid curves show the best fits (see text). The measured γ-ray transitions are indicated in the figure.

Fig. 8. Out-of-plane angular distributions of discrete γ-rays from $^{162-x}Dy$ ($4 \leq x \leq 6$) measured in coincidence with α-particles emitted at 60° in the $^{159}Tb(^{7}Li, xn)^{162-x}Dy$ reaction at 77 MeV. The solid curves show the best fits (see text). The measured γ-ray transitions are indicated.

Fig. 9. Energy spectra of protons, deuterons, tritons, and α-particles observed at 20° measured in coincidence with fission fragments taken in and out of the reaction plane in the $^{232}Th + ^{7}Li$ reaction at 77 MeV.

Fig. 10. In-plane and out-of-plane angular distributions of fission fragments measured in coincidence with protons, deuterons, tritons, and α-particles emitted at 20° in the $^{232}Th(^{7}Li,xf)$ (x = p,d,t,α) reaction at 77 MeV. The solid curves show the best fits obtained by method A (see text) with K_o = 10 ħ for α-particles and K_o = 11 ħ for protons, deuterons, and tritons. The sensitivity of the fit on J is indicated by dashed and dotted-dashed curves in the figures; the solid curves are obtained with (J,J_2) = (25,24) for protons, (J,J_2) = (21,20) for deuterons, (J,J_2) = (16,12) for tritons, and (J,J_2) = (16,9) for α-particles. The dotted-dashed curves are obtained with (J,J_2) = (26,25) for tritons and (J,J_2) = (24,20) for α-particles. The angular momenta J and J_2 are given in units of ħ.

Fig. 11. Angular momenta transferred to the fissioning nucleus as a function of the ejectile masses in the $^{232}Th(^{7}Li,xf)$ (x = p,d,t, or α) reaction at 77 MeV.

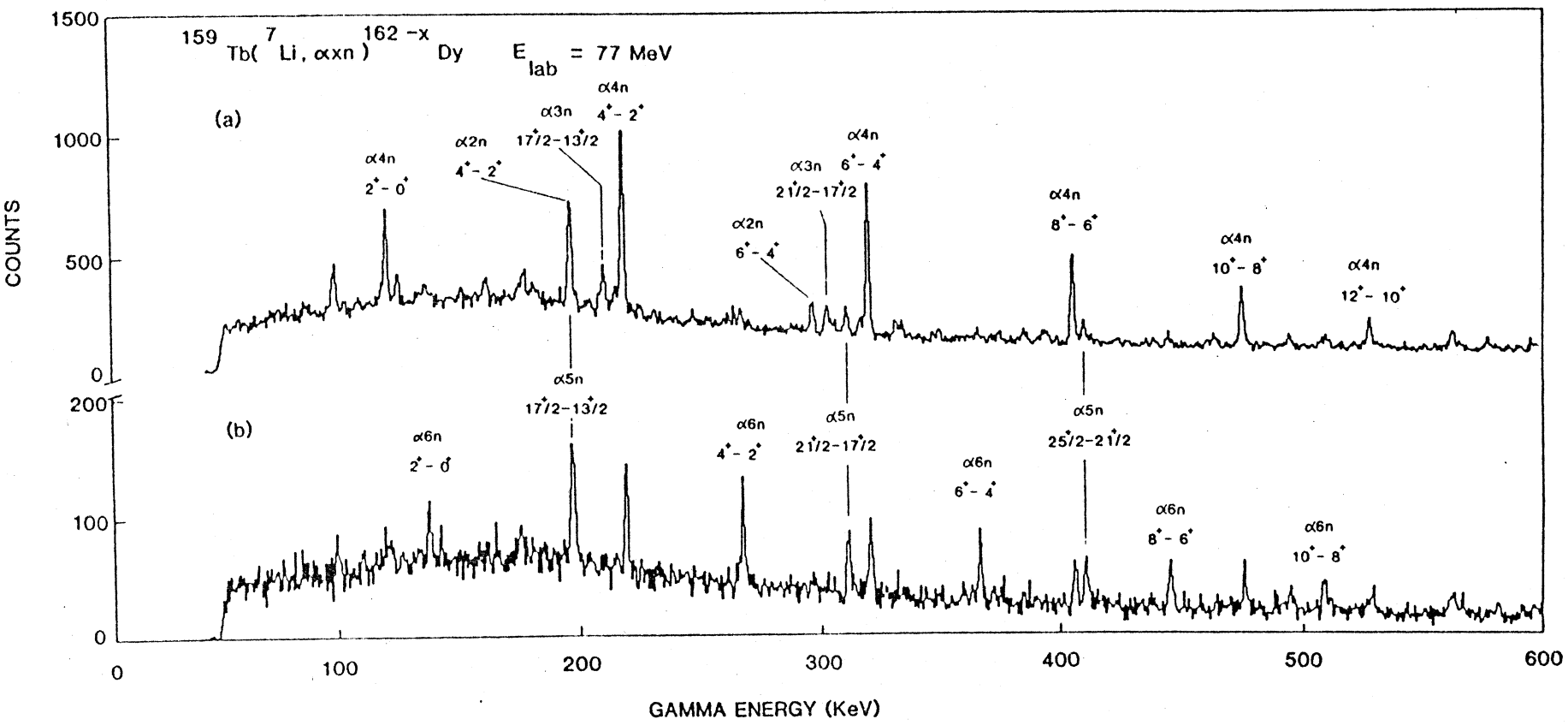
159 Tb(7 Li, αxn) 162 -x Dy E lab = 77 MeV
(a)
(b)
α4n 2+ - 0+
α2n 4+ - 2+
α3n 17/2+ - 13/2+
α4n 4+ - 2+
α2n 6+ - 4+
α3n 21/2+ - 17/2+
α4n 6+ - 4+
α4n 8+ - 6+
α4n 10+ - 8+
α4n 12+ - 10+
α5n 17/2+ - 13/2+
α6n 2+ - 0+
α6n 4+ - 2+
α5n 21/2+ - 17/2+
α6n 6+ - 4+
α5n 25/2+ - 21/2+
α6n 8+ - 6+
α6n 10+ - 8+
COUNTS
GAMMA ENERGY (KeV)
0
100
200
300
400
500
600
500
1000
1500
100
200

Fig. 1

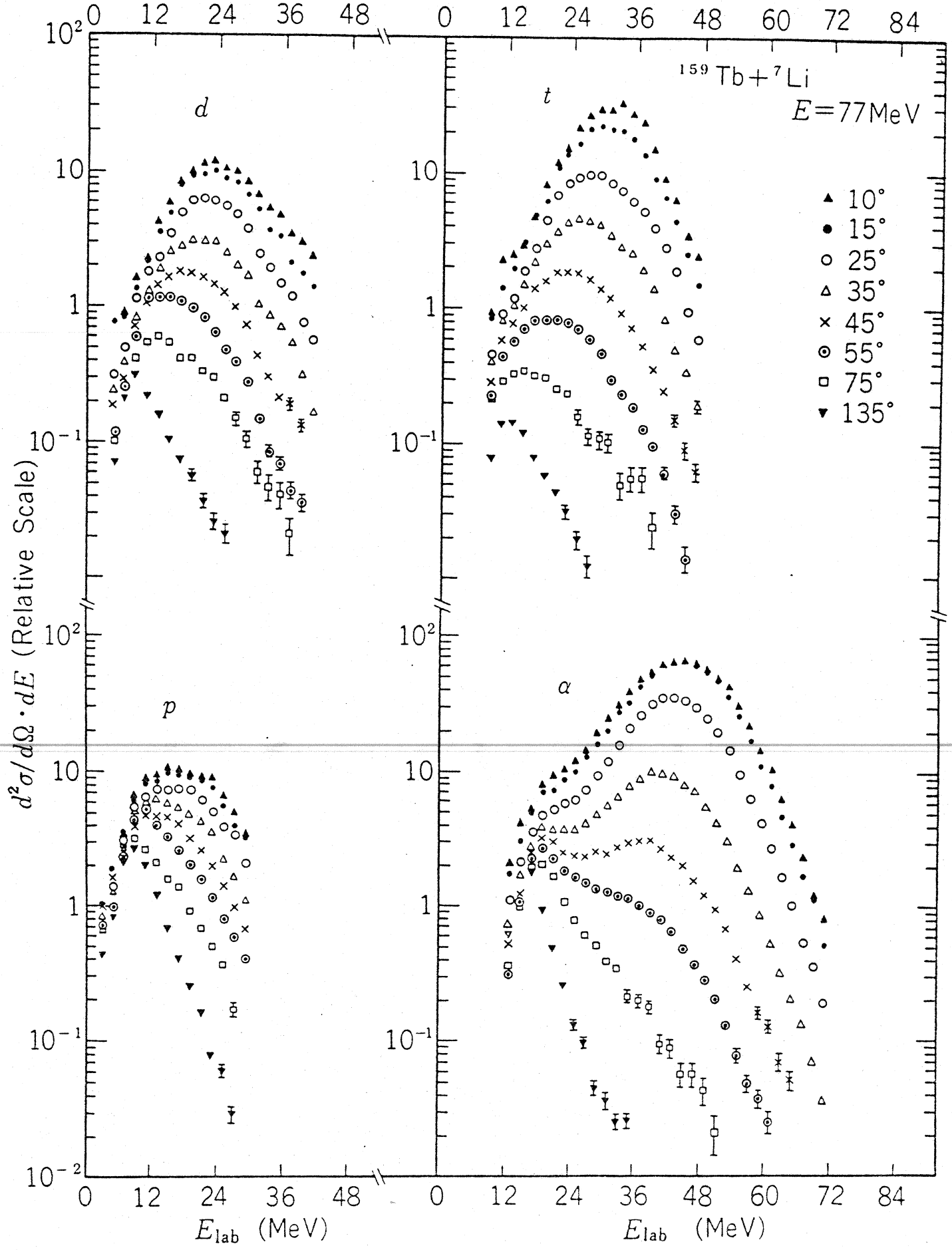
^{159}Tb+^{7}Li
E=77MeV
d
t
p
α
10°
15°
25°
35°
45°
55°
75°
135°
$d^2\sigma/d\Omega \cdot dE$ (Relative Scale)
E_{lab} (MeV)
E_{lab} (MeV)

Fig. 2

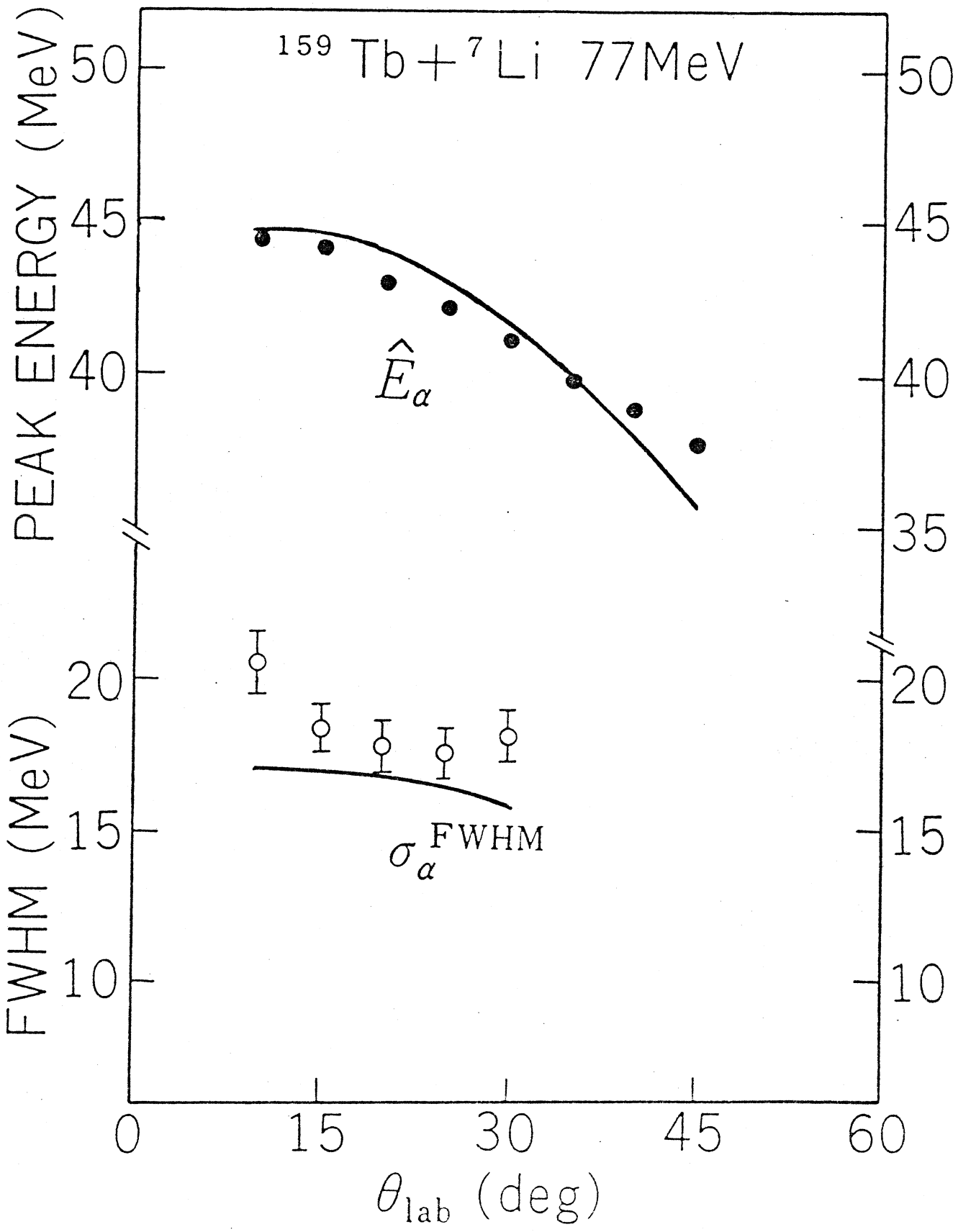
^{159}Tb + ^{7}Li 77MeV
PEAK ENERGY (MeV)
FWHM (MeV)
$\hat{E}_\alpha$
$\sigma_\alpha^{\mathrm{FWHM}}$
50
45
40
35
20
15
10
0
15
30
45
60
θ_{lab} (deg)

Fig. 3

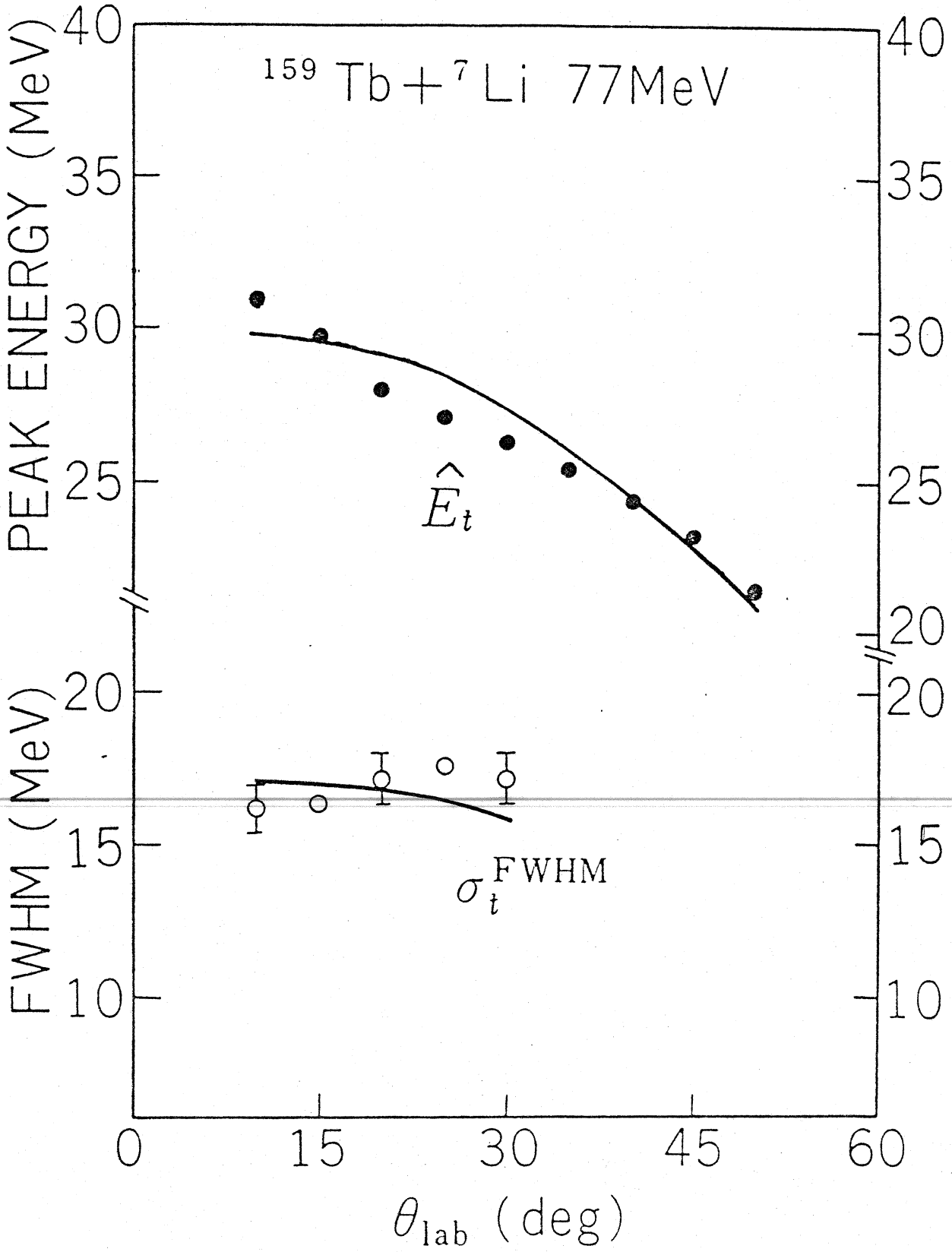
^{159}Tb + ^{7}Li 77MeV
PEAK ENERGY (MeV)
FWHM (MeV)
$\hat{E}_t$
σ_t^{FWHM}
θ_{lab} (deg)
40
35
30
25
20
15
10
0
15
30
45
60

Fig. 4

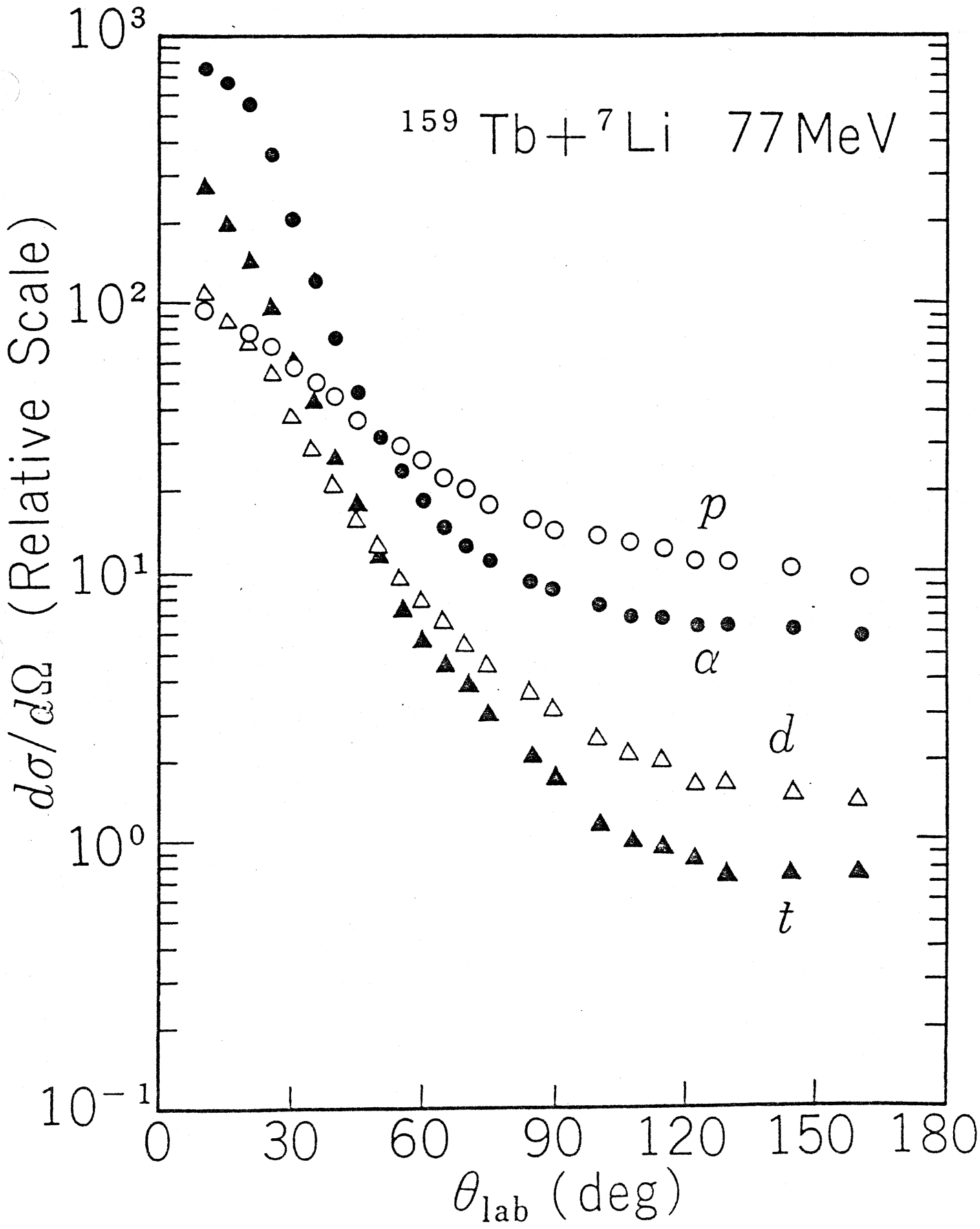
^{159}Tb+^{7}Li 77MeV
$d\sigma/d\Omega$ (Relative Scale)
10^3
10^2
10^1
10^0
10^{-1}
0
30
60
90
120
150
180
θ_{lab} (deg)
p
α
d
t

Fig. 5

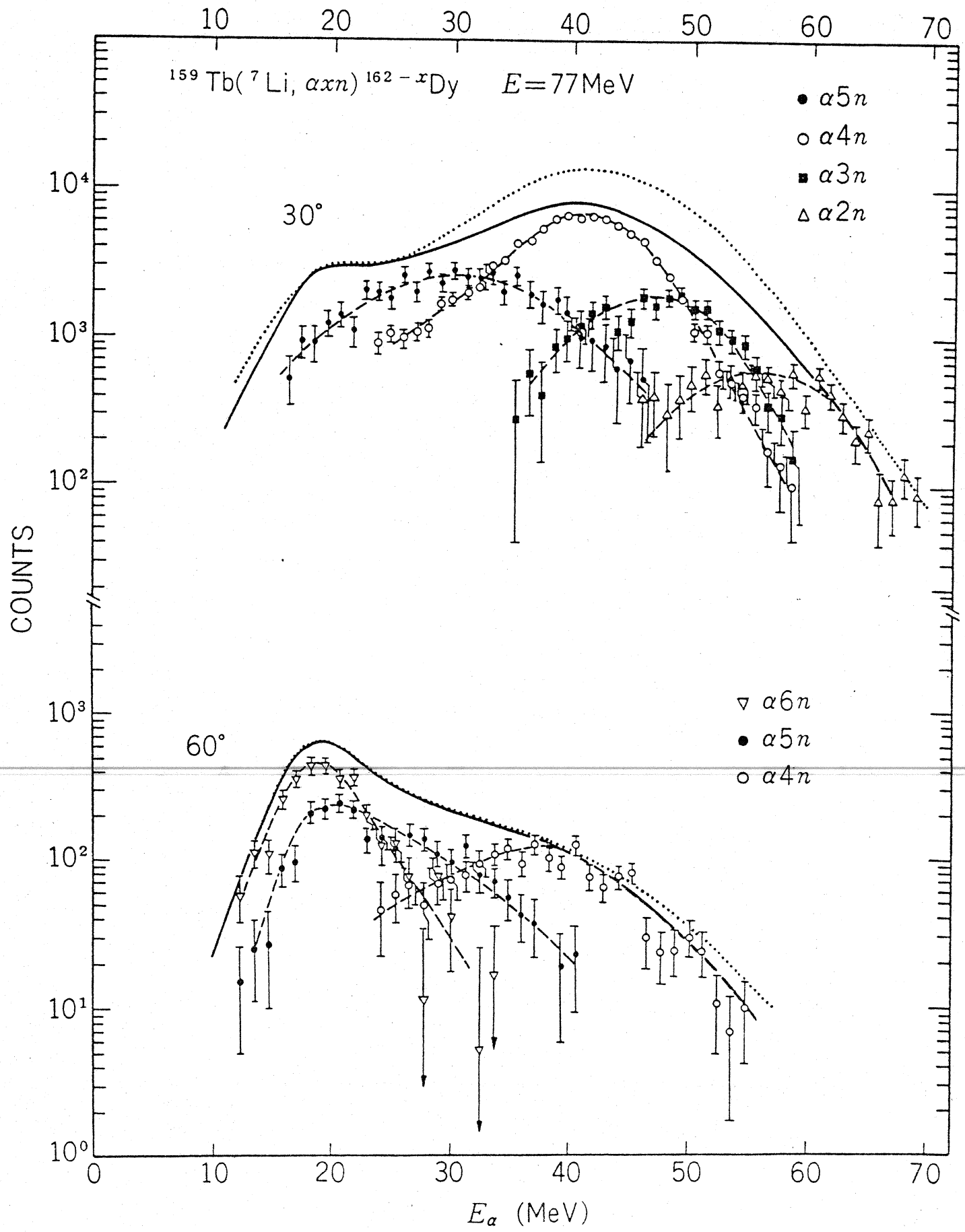
^{159}Tb(^{7}Li, αxn)$^{162-x}$Dy E=77MeV
$\alpha 5n$
$\alpha 4n$
$\alpha 3n$
$\alpha 2n$
30°
$\alpha 6n$
$\alpha 5n$
$\alpha 4n$
60°
COUNTS
E_α (MeV)

Fig. 6

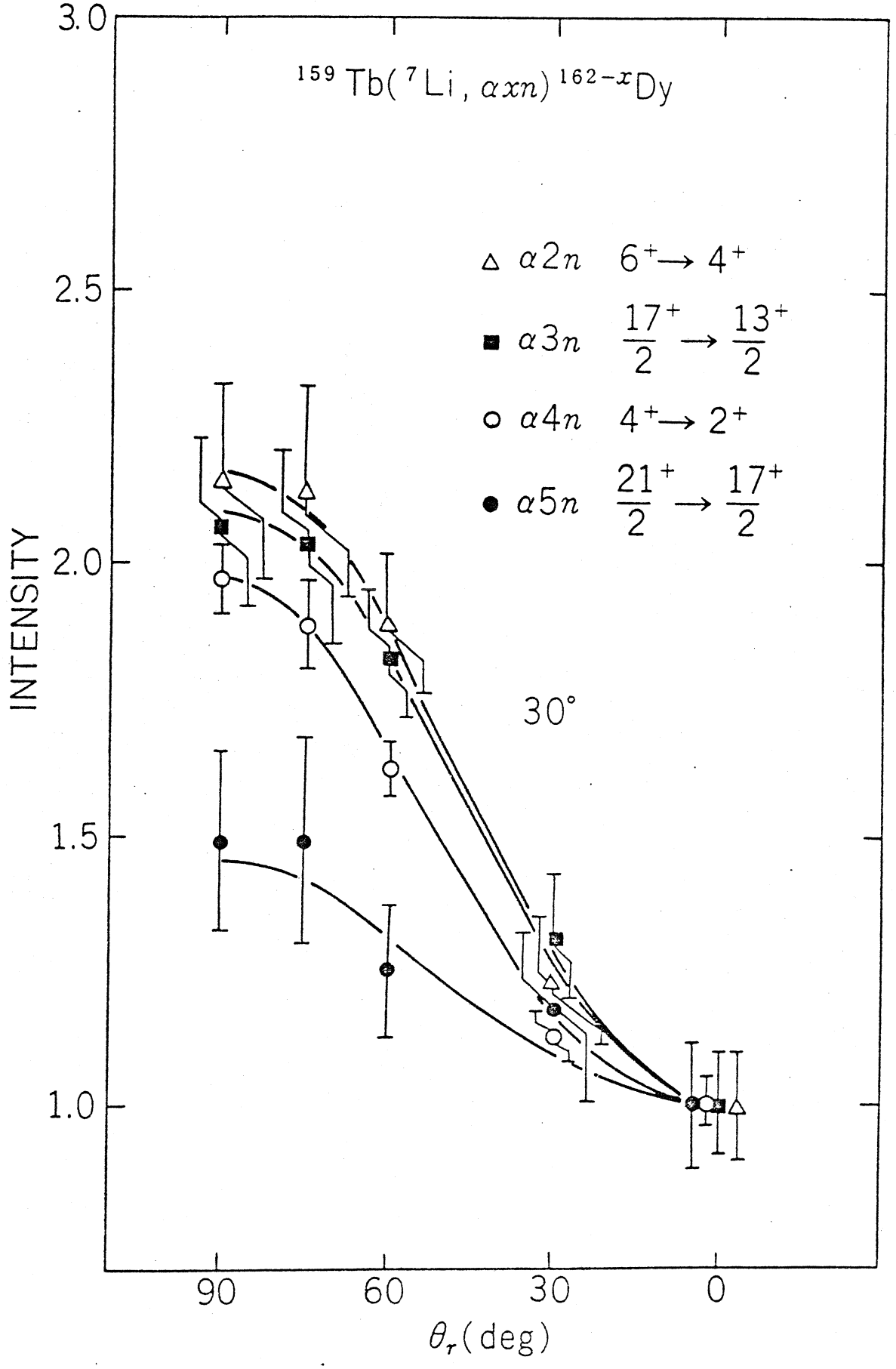
$^{159}Tb(^{7}Li, \alpha xn)^{162-x}Dy$
△ α2n 6⁺ → 4⁺
■ α3n 17⁺/2 → 13⁺/2
○ α4n 4⁺ → 2⁺
● α5n 21⁺/2 → 17⁺/2
30°
INTENSITY
3.0
2.5
2.0
1.5
1.0
90
60
30
0
θr (deg)

Fig. 7

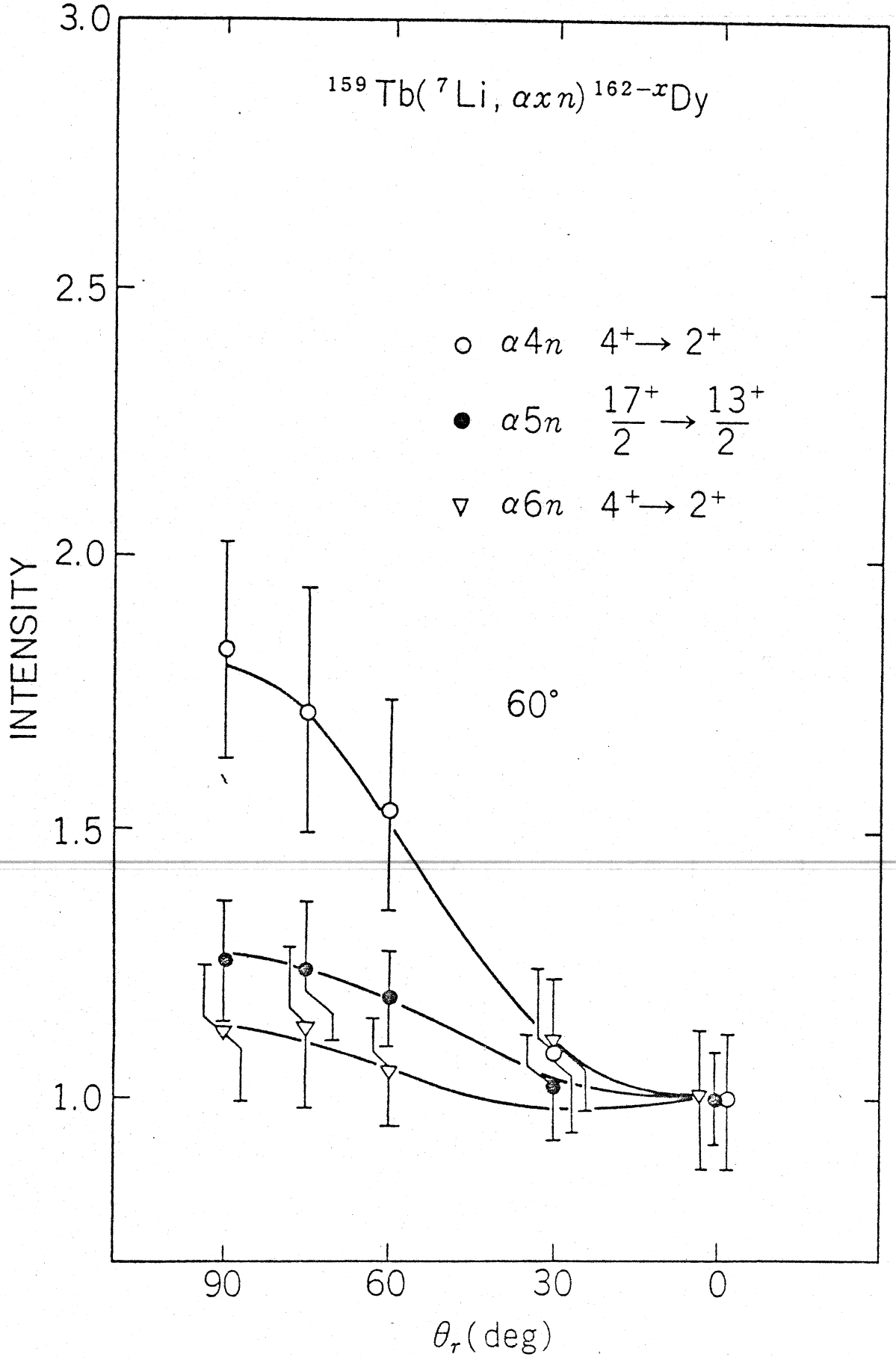
$^{159}Tb(^{7}Li, \alpha x n)^{162-x}Dy$
○ α4n 4⁺ → 2⁺
● α5n 17⁺/2 → 13⁺/2
▽ α6n 4⁺ → 2⁺
60°
INTENSITY
3.0
2.5
2.0
1.5
1.0
90
60
30
0
θ_r (deg)

Fig. 8

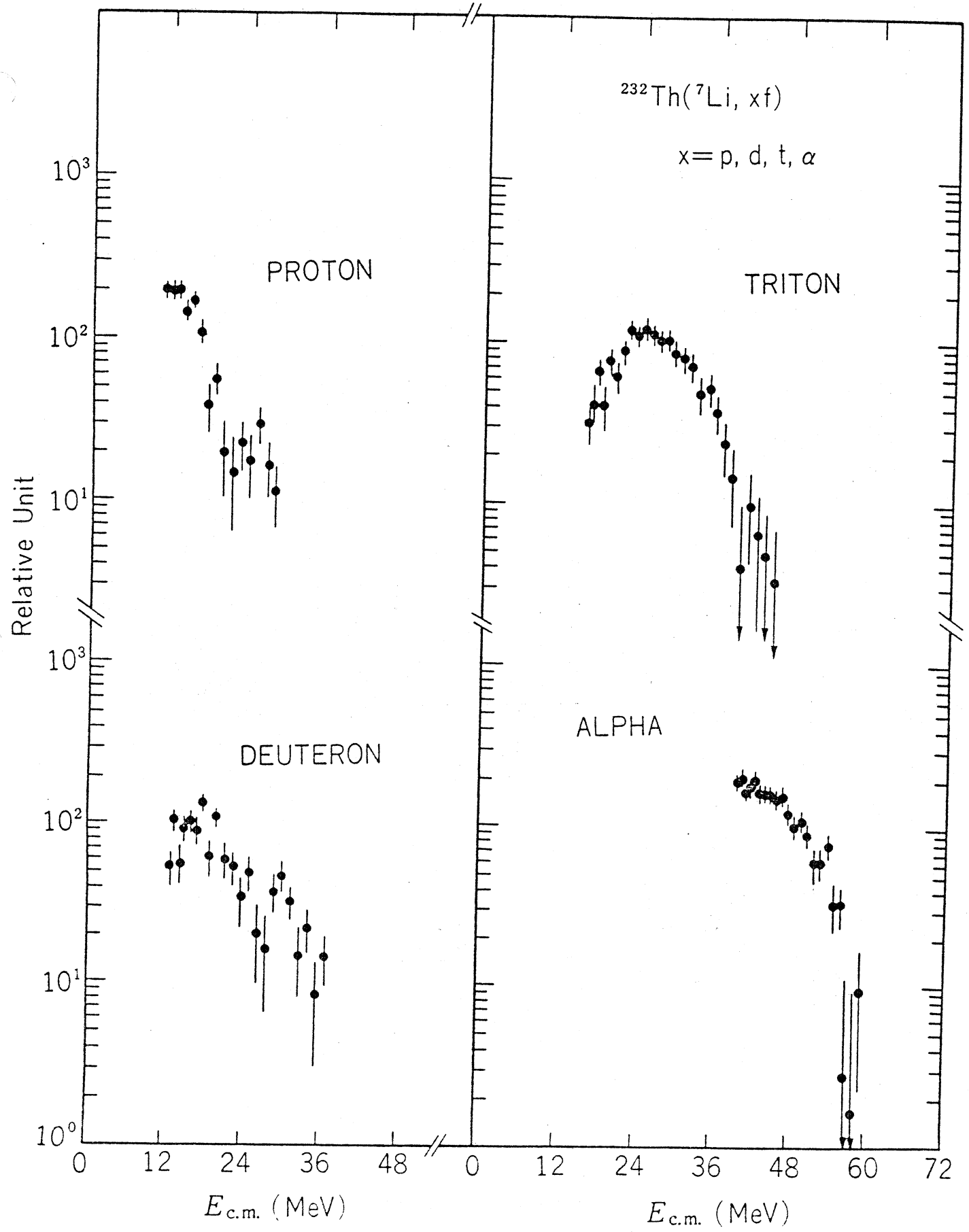
^{232}Th(^{7}Li, xf)
x= p, d, t, α
PROTON
TRITON
DEUTERON
ALPHA
Relative Unit
10^3
10^2
10^1
10^0
0
12
24
36
48
60
72
$E_{c.m.}$ (MeV)
$E_{c.m.}$ (MeV)

Fig. 9

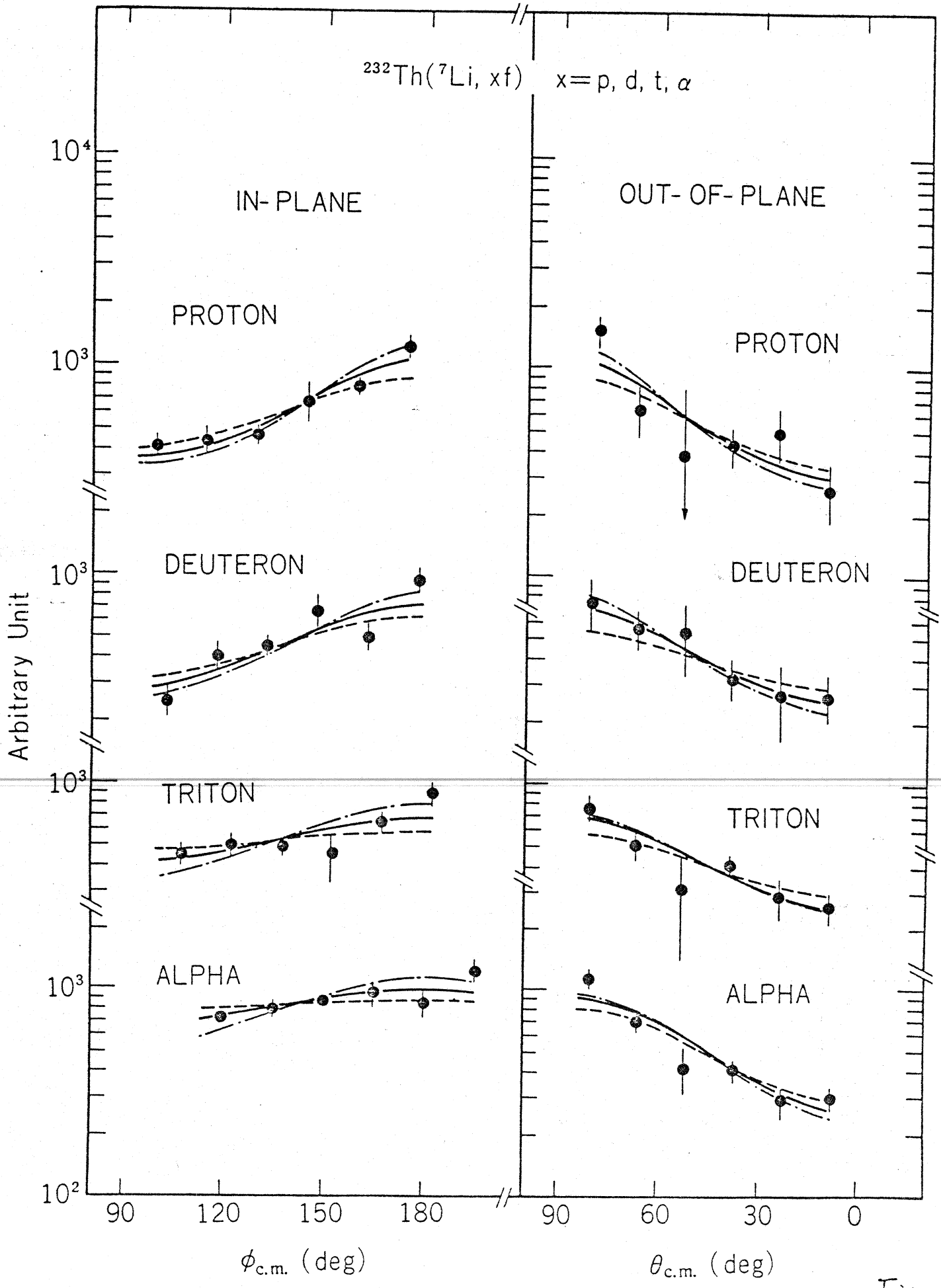
^{232}Th(^{7}Li, xf) x = p, d, t, α
IN-PLANE
OUT-OF-PLANE
PROTON
DEUTERON
TRITON
ALPHA
Arbitrary Unit
10^4
10^3
10^2
90
120
150
180
60
30
0
$\phi_{c.m.}$ (deg)
$\theta_{c.m.}$ (deg)

Fig. 10

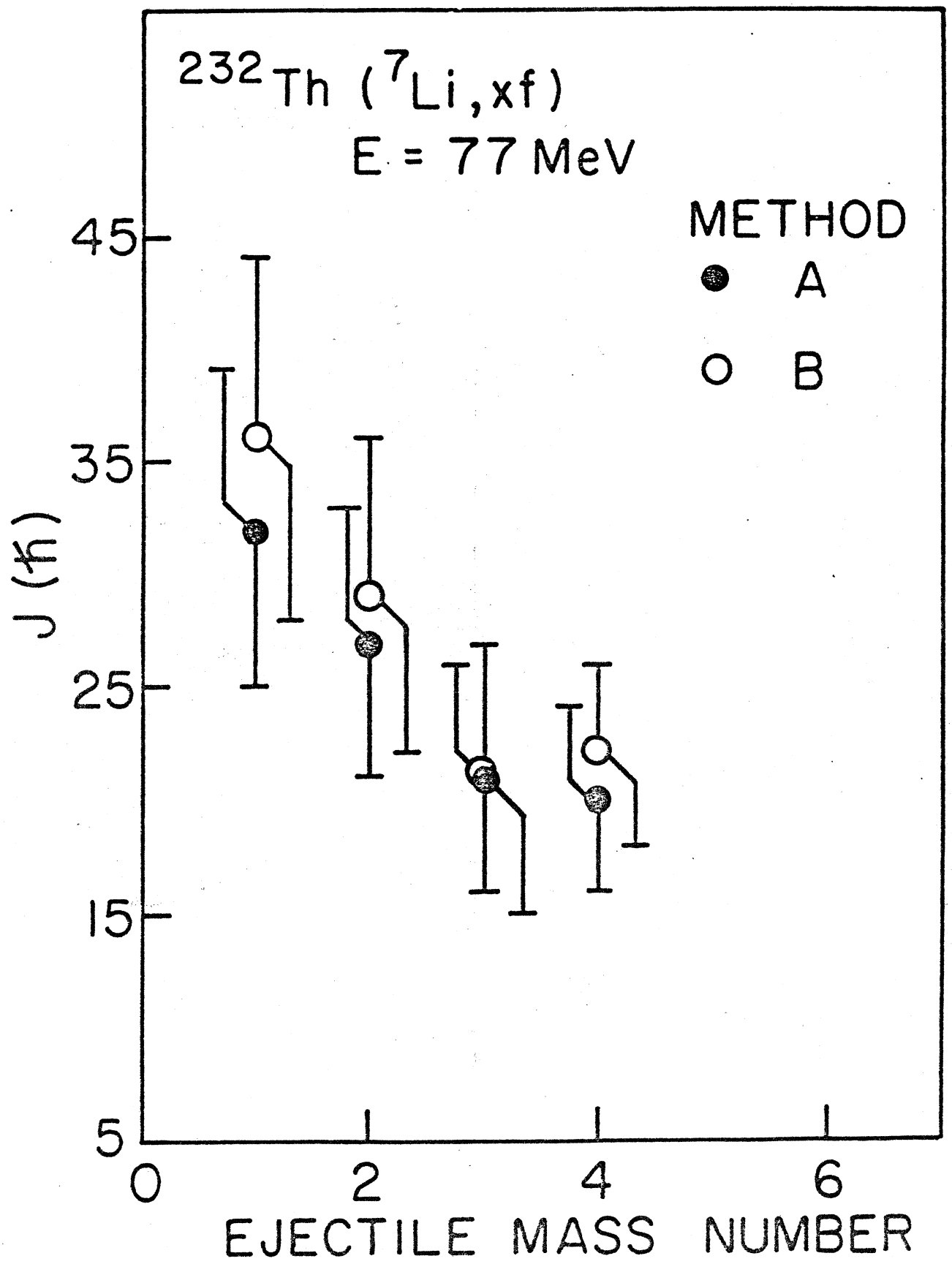
^{232}Th (^{7}Li, xf)
E = 77 MeV
METHOD
A
B
45
35
25
15
5
J (ħ)
0
2
4
6
EJECTILE MASS NUMBER

Fig. 11